The Anhydrous Regolith of the Moon

R. R. Hodges* **and W. M. Farrell†**

Key Points:

- The upper limit for water in the lunar exosphere is ~ 3 molecules/cc.
- The lunar exosphere does not transport water to polar cold traps.
- Lunar regolith is anhydrous.

*Laboratory for Atmospheric and Space Physics, University of Colorado, Boulder, Colorado, USA.
†NASA Goddard Space Flight Center, Greenbelt, MD, USA

Corresponding author: R. R. Hodges, hodges@lasp.colorado.edu

Abstract

The hypothesis that significant deposits of water ice exist in cold traps near lunar poles includes a supposition that acquired water is concentrated in the traps by exospheric lateral transport. That supposition, and by inference the trapped water hypothesis, are proven to be false by the present analysis of data obtained in 2013-2014 by the neutral mass spectrometer on the Lunar Atmosphere and Dust Environment Explorer (LADEE) spacecraft. These data show no evidence of exospheric water. The upper limit for exospheric water at the lunar surface, ~ 3 molecules cm^{-3}, is deficient by several orders of magnitude in accounting for the deposition of the chondritic influx of water in cold traps. The present hypothesis is that the precursor of clay formation, cation exchange involving water molecules and anorthite, is analogous to reversible chemi-sorption, and that adsorbed water on the lunar surface is rapidly removed from the moon by solar wind sputtering.

Plain Language Summary

Whether vast deposits of water ice has accumulated in lunar polar cold traps hinges on an unproven hypothesis that water acquired mainly from meteorites (and possibly from other sources as well) at a rate of about 5 tonnes per year, is moved to polar cold traps by the dynamic transport process of the lunar exosphere (a rarefied, collisionless atmosphere). Movement of exospheric molecules over the lunar surface is a 2-dimensional random walk process in which the steps are random segments of Kepler trajectories that begin with thermal desorption from soil grains and end with adsorption at distances measured in hundreds of kilometers; obviously, trajectories that end in cold traps must create ice deposits. However, the upper bound for exospheric water derived here from data collected in 2013-2014 by the neutral mass spectrometer on the Lunar Atmosphere and Dust Environment Explorer spacecraft, about 3 molecules/cc, pales in comparison to the concentration of $\sim 15,000$ molecules/cc needed to sequester the meteoritic water influx. The only pragmatic conclusion is that the hypothesis for water ice accumulation at the poles due to exospheric transport is false. This conclusion forces the question of the fate of water that accretes on the lunar surface.

1 Introduction

Optimism about resource level abundances of water sequestered near the lunar poles stems mainly from a reasonable hypothesis of Watson et al. (1961) and a more focussed discussion by Arnold (1979) about how water acquired from external and internal sources could have been concentrated in polar cold traps by exospheric transport processes. A simplistic description of the lunar exosphere is a collisionless atmosphere where molecules travel randomly from point to point on the surface via ballistic trajectories that are segments of Kepler orbits. Upon impacting the regolith surface of the moon, exospheric molecules tend to do a 3-dimensional random walk among soil grains, each encounter involving adsorption followed by thermally controlled desorption and thermal departure either to another grain or back into the exosphere. If photolysis and surface chemistry could be neglected it would be inevitable that the exospheric lifetimes of water molecules would end in cold traps and create ice.

However, the elephant in the room is argon-40 sorption, an issue that has been known and, like Krylov's Inquisitive Man, ignored for decades. The diurnal variation of inert gases at the lunar surface was predicted by Hodges and Johnson (1968) to approximate the classic $T^{-5/2}$ law of exospheric equilibrium. For the moon, that translates to a night to day ratio of about 30:1. That expectation was shattered in the data from the first hour of operation of the Apollo 17 neutral mass spectrometer (Hodges et al., 1973): argon-40 mimics the behavior envisioned by Hodges and Johnson for water vapor, that is, depletion at night due to condensation and a sunrise bulge as the surface warms.

The activation energy for desorption required to remove argon from the nighttime lunar exosphere is about 6 kJ/mole (Hodges, 1980, 1991, 2002). This level can only occur on pristine, water-free surfaces (Bernatowicz & Podosek, 1991). While the Apollo 17 data relate only to low latitudes, the identification of a seasonal oscillation of argon-40 in the lunar atmosphere (Hodges & Mahaffy, 2016) extends the pristine soil requirement into lunar polar regions.

In practical terms, surfaces of soil grains over nearly all of the lunar surface, including polar regions, are limited to significantly less than one monolayer of water. Implicit in this assertion is that without adsorbed water, experimental studies involving rehydration of returned soil samples are not relevant to the global water issue.

This report begins with the derivation of an upper bound for lunar exospheric water based on data collected by the neutral mass spectrometer (NMS) on the Lunar Atmosphere and Dust Environment Explorer (LADEE) spacecraft. The discussion progresses to an explanation of why water, assimilated globally, is not moved to cold traps by exospheric lateral transport as proposed by Watson et al. (1961) and Arnold (1979). Subsequent discussion centers on global processes for removal of incoming water fast enough to avoid creating a detectable exospheric signature while avoiding the sub-monolayer limit imposed by argon sorption observations.

2 The Upper Limit for Exospheric Water

The data that form the basis for this discussion were acquired by the neutral mass spectrometer (NMS) on the LADEE spacecraft (Mahaffy et al., 2014). These measurements are contaminated by artifact water and methane created in a getter by gases evolving from the hot filament of the ion source (Hodges, 2016). Ironically, the getter was installed in the mass analyzer for vacuum maintenance, facilitating the inclusion of a mass spectrum in pre-flight and post-launch verifications of the operational status of the NMS. The extraction of an exospheric component of methane from the compromised data is explained in Hodges (2016), and an obvious correlation of water and the artifact component of methane is discussed in Hodges (2018).

Among the neutral mass spectra acquired by LADEE there are 394 orbits, spread over 140 days, wherein the mode of operation provided repetitious, paired monitoring of water and methane beginning around local noon, traversing the sunrise terminator, and ending around local midnight. Salient facts about this data set include that the orbit was retrograde with periapsis near the sunrise terminator to sample the highest concentrations of minor species in the classic sunrise bulge of exospheric gases (Hodges & Johnson, 1968). Spacecraft battery capacity restricted operation of the NMS to 1/2 of an orbit each time it was powered. Resource sharing further limited usage of the NMS to a few orbits per day. Owing to the inability of the mass analyzer to separate the 16 amu mass defects of methane and atomic oxygen, the unencumbered CH_3 fragment of methane at 15 amu is used here as a proxy for methane. The unit of measure is counts per integration period (247 ms) after applying the standard adjustment for thermo-molecular pressure difference (Mahaffy et al., 2014).

Paired measurements of H_2O and CH_3 from each of the 394 orbits that meet modal criteria have been averaged in one hour local time (LT) zones, condensing the data to one point per orbit per LT hour (about 4.6 minutes of instrument time). These points are presented in Figure 1 as color-coded scatter plots. The format is H_2O versus CH_3, with abscissas shifted by $\sqrt{10}$ in successive time zones. The order of plotting data points is randomized to keep late orbits from overwhelming early ones and obscuring color trends. LT boundaries are annotated at the top of each LT collection of data points and the corresponding scale factor of abscissas is at the bottom. Owing to the retrograde orbit of

the spacecraft, LT decreases from left to right as operating time of the instrument increases. Trend lines are intended only to guide the eye.

In panel A of Figure 1 there are two identical sets of local time zone scatter plots of raw data points. The upper row is color-coded in days measured from 1 January 2014; color-coding in the lower row is according to spacecraft altitude. What immediately meets the eye is the stratifications of colors in the upper row, and the lack thereof in the lower row. If water and methane were both atmospheric constituents, the altitude identification colors in the lower row would progress upwards barometrically from blue to red. On the other hand, the well-defined rainbow patterns in the upper row of scatter plots are consistent with an instrumental process that created artifact water and methane with steadily decreasing efficiency over the duration of the mission (Hodges, 2018).

Inasmuch as methane is (and by inference, water must be) depleted in lunar nighttime due to adsorption on cold soil grains, neither natural water nor methane could have contributed to the measurements in the 00-05 LT zones (which are combined in the scatter plots). In other words, this set of data points is entirely instrumental artifact. It follows that the nature of the instrumental process that created these artifacts can be derived from the 00-05 data collection. The rainbow effect, the general power-law trend of the data, and a less obvious, but important, difference in the trends of red and blue dots, suggest that the artifact generating process can be approximated empirically by

$$[\mathrm{H_2O}] = \eta_{orbit} G(t) F([\mathrm{CH_3}])^P \tag{1}$$

where $G(t)$ is a LT-dependent scale factor, and the coefficient η accounts for orbit-to-orbit variations in the feedstock of the instrumental process that creates CH_4 and H_2O. The function F is

$$F(X) = \mathrm{e}^{\alpha D} X^{1+\beta D} \tag{2}$$

where D is fractional time in days measured from the start of year 2014, the first term is the correction for the rainbow effect while the second term corrects for a systematic perturbation of the power law of the process. Coefficients derived from a least square error fit of equation 1 to the 00-05 hour data collection are: $\alpha = 0.01177$, $\beta = -0.001559$, and $P = 2.446$.

In panel B of Figure 1 the scale of abscissas is transformed from raw data counts to the temporal function $F([\mathrm{CH_3}]_{\mathrm{lad}})$. The validity of the transformation function F is supported by the way that almost two thousand nighttime data points cling to the 00-05 LT regression line. In daytime the scatter of the dots is probably owed to variations of rates of filament out-gassing of the feedstock components of the artifact-generating processes, rates that are influenced by randomness in previous periods of annealing of the filament surface each time power was removed at the end of about an hour of NMS operation (Hodges, 2018).

In daytime hours of panel B the methane correction of abscissas tends to align dots parallel to regression lines at high artifact levels but curve downward at the low end. This is caused by the barometric distribution of natural exospheric methane. In panel C, the diurnal methane simulation of Hodges (2016), scaled to a global supply rate of $4{\times}10^{21}$ molecules per second and converted to detector counts, has been subtracted from the raw data before application of the abscissa transformation. The resulting conformance of all residual daytime data with trend lines and the absence of a barometric decay with altitude is ample proof that water in LADEE data is artifact.

Figure 2 shows the results of converting detector counts for H_2O to exospheric concentrations as described in Mahaffy et al. (2014), and then extrapolating them barometrically to the lunar geoid to identify the lowest concentration in each LT group. These data points are absolute upper bounds for water concentration at the geoid. However, it is apparent in Figure 1 that if the exospheric contribution near noon were 50% at lowest altitudes, the nature of the distribution of dots would be noticeably different. In other

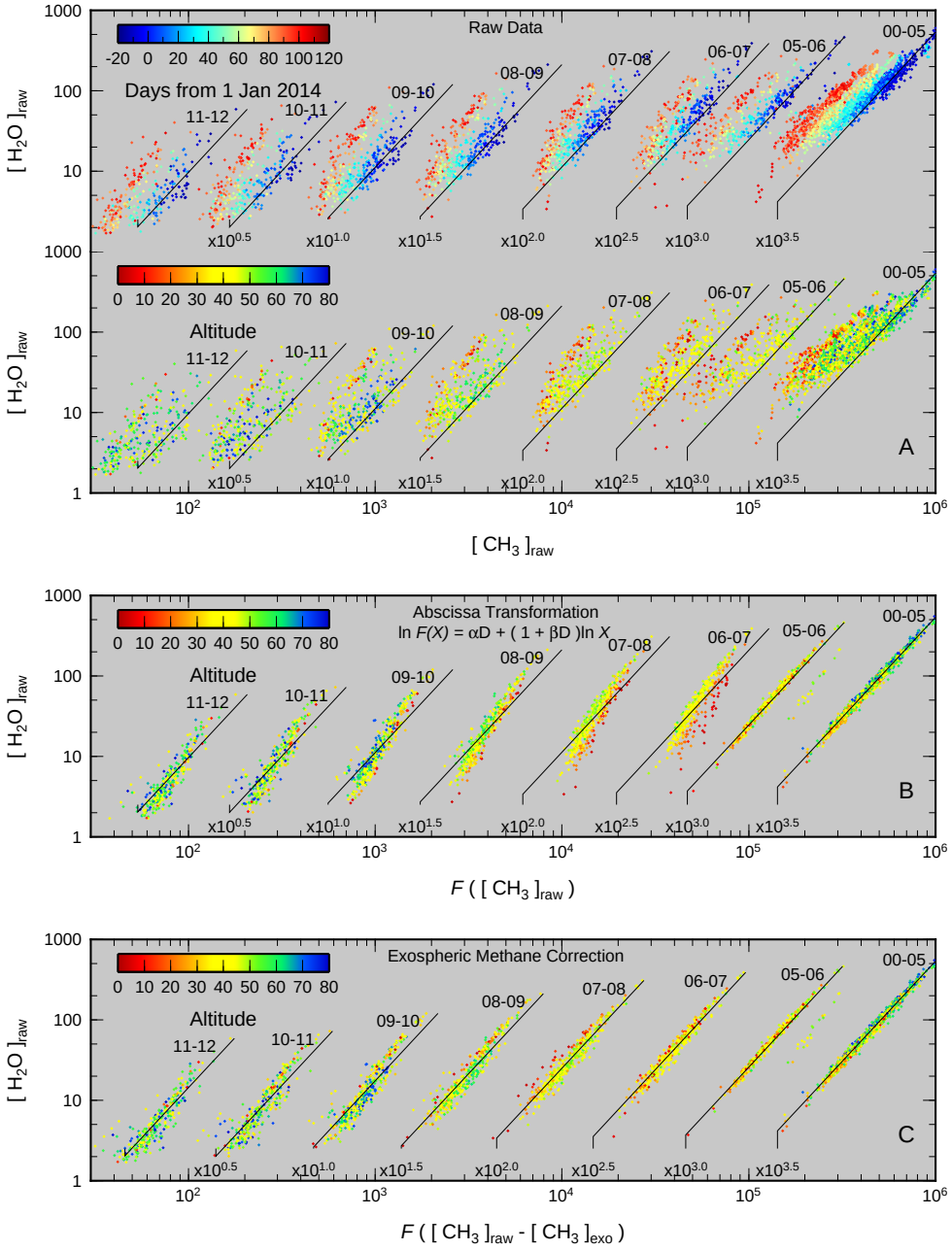

Figure 1. Scatter plots of LADEE mass spectrometer measurements of water versus the methane proxy CH_3 from a set of 394 orbits wherein NMS power-on occurred within ±7.5°of longitude from the sub-solar meridian and ended near nadir (the orbit is retrograde). The unit is detector counts per 237 ms. Coordinates of each data point represent the time averages of 13 to 80 paired measurements in a 1 hour local time (LT) interval. Trend lines are included to guide the eye; LT is at the top of each trend line and abscissa scale offset is at the bottom. Panel A: Raw data color coded according to time in days from 1 January 2014 (top), and according to spacecraft altitude (bottom). Panel B: Raw dated re-plotted with the abscissa transformed by equation 2. Panel C: CH_3 corrected for exospheric methane and transformed by equation 2.

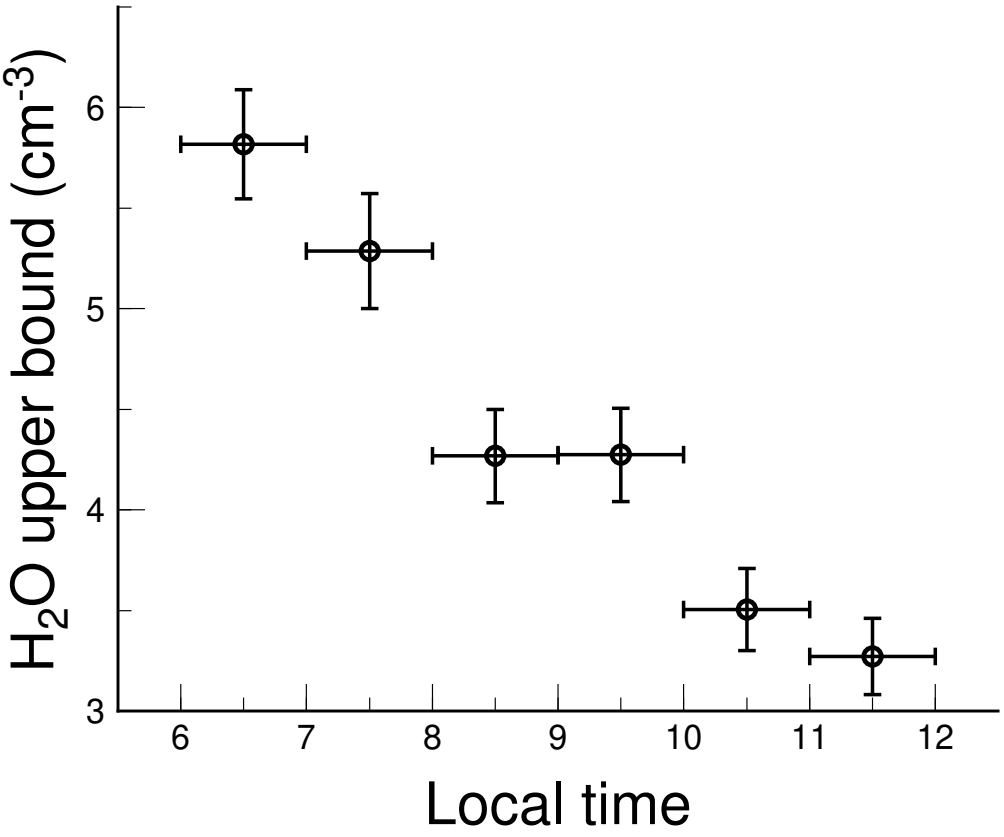

Figure 2. Absolute upper limits for exospheric water vapor concentrations at the lunar geoid. These data exaggerate true upper limits by at least a factor of 2.

words, Figure 2 exaggerates the upper limit for exospheric water by at least a factor of 2.

3 Discussion

The only steady source of lunar water to have survived scrutiny among those posited by Arnold (1979) is carbonaceous chondrites. Borin et al. (2017) estimate that 3.66×10^9 g of meteoritic material impact the moon each year. Continuing with Arnold's presumption that the average abundance of water in chondritic meteorites is 3%, and assuming that carbonaceous chondrites account for 4.6% of the meteoritic infall (Bischoff & Geiger, 1995), the rate of water acquisition by the moon should amount to at least 5×10^6 g/A, which is also the lower bound of Arnold's estimate of water acquisition.

To view the upper bounds of Figure 2 in lunar perspective, suppose that the exospheric water transport process were to exist under most favorable conditions: that the exosphere is Maxwellian, that cold traps cover as much as 5% of the lunar surface at latitudes above 80°, that all exospheric water molecules falling on cold traps become ice, and that sublimation of trapped ice is negligible. For the cold traps to sequester water at the global accretion rate, $\sim 5\times10^6$ g/A, the product of the total trap area and the Maxwellian flux of exospheric water molecules striking the lunar surface near the poles would have to equal the global water accretion rate. Assuming an average surface temperature of 200K in polar regions, the total trapping of water molecules would require an exospheric water concentration of $\sim 3,000$ molecules cm^{-3}. That level is approxi-

mately independent of latitude because the tendency toward exospheric equilibrium (i.e., surface concentration varies approximately as $T^{-5/2}$; cf. Hodges & Johnson, 1968) is effectively cancelled by the diffusive nature of poleward exospheric transport (Hodges, 1972). In other words, there is a 3 order of magnitude difference between incoming water and polar ice creation. This discrepancy begs the question: What happens to 5×10^6 g of meteoritic water that is accreted by the moon each year?

3.1 Accretion of meteoritic water

Meteorites impact the moon at speeds capable of vaporizing themselves and surrounding lunar material at a rate of 1.8×10^{-15} g cm^{-2} s^{-1} (Cremonese et al., 2013). Vapor temperatures that are great enough to cause significant escape (i.e., greater than 5000 K) are unlikely. Instead, the mean speed of molecules increases with adiabatic expansion, the vapor becomes collisionless, and, even at melt temperatures ($\sim$ 2000K), the vapor is ballistically dispersed over an area of hemispheric dimensions, with each molecule following an independent, planetary scale Keplerian trajectory.

The result is a constant "rain" of water (and mineral) molecules over the entire lunar surface. Ignoring direct escape and inflight-photolysis, the global average rain of water molecules should approximate the water component of the meteoritic influx, that is, $\sim 14,000$ molecules cm^{-2} s^{-1} (based on estimates discussed above). With impact vapor temperatures around 2000K the average concentration of water in the molecular rain should be less than 0.4 cm^{-3}.

In the reports of Epstein and Taylor (1971, 1972, 1973, 1974, 1975) on the pyrolysis of soil samples from all Apollo sites, the extraction of water generally begins around 400C. In the range of roughly 400-600C all of the extracted water has the isotopic characteristics of terrestrial water acquired during or after sample collection. At temperatures above 600C the isotopic pattern shifts toward deuterium-depleted lunar water that is created in laboratory apparatus from extracted solar wind hydrogen. It is important to note that this pattern is inherent in surface samples as well as all 3 sections of the Apollo 15 deep core.

3.2 Water sorption

The absence of indigenous water in the lower section of the Apollo 15 core indicates that when meteoritic water molecules fall on the regolith surface they do not diffuse into the regolith by grain to grain migration, even over GA time scales. In other words, the activation energy for desorption on the regolith surface is sufficient to keep H_2O molecules immobilized long enough to allow them to be annihilated by dissociation or to escape before a monolayer forms. The nature of removal mechanisms restricts the sorption process to exposed grain surfaces.

Lunar soil grains are coated with thin ($\sim$ 200 nm) rims of amorphous material (Bibring et al., 1972) of uncertain composition that is a byproduct of space weathering. One unexplored possibility, that can explain both the existence of the rims and the relatively high activation energy required to retain water up to 400-600C, is that the rims are phyllosilicates (e.g., clay) created by gradual weathering of anorthite by water.

When liquid water meets anorthite, the initial result is the progenitor of clay, reversible Ca-H cation exchange. It is obvious that clay cannot be created by an isolated water molecule adsorbed on anorthite. However, at the molecular level, the precursor of the clay-forming bond, Ca-H exchange, is a reversible chemi-sorption process. Over time, some clay-like phyllosilicates should have accumulated whenever monolayer coverage was approached and adsorbed water molecules began to cluster in adjacent adsorption sites.

In this scenario, any water molecule released at micro-meteoroid impact would then undergo one ballistic trajectory of global scale and then be chemi-adsorbed by the surface. It should be noted that a similar scenario of cation exchange occurs when water meets forsterite. In addition, both process create hydrated phyllosilicates that possibly provide the OH in lunar soils reported by Clark (2009), Pieters et al. (2009), and Sunshine et al. (2009).

3.3 Water removal

Possibilities for removal of water from the moon are limited to annihilation and escape. Intuitive mechanisms include photolysis and solar wind sputtering. However, the anhydrous nature of the regolith imposed by argon desorption, the absence of adsorbed indigenous water in returned soils, and the paucity of experimental and/or theoretical guidance for the rate of photolysis of individual water molecules adsorbed on a grain surface, make photodissociation difficult to defend.

Housley (1977) suggested that cleansing of regolith grain surfaces and forced escape of extra-lunar contaminants occurs naturally as a result of solar wind bombardment. The nominal solar wind flux is $\sim 3{\times}10^8$ cm^{-2} s^{-1}. Diurnal averaging and solar wind blockage during the periodic passage of the Moon through the geomagnetic tail reduce the average equatorial influx to $\sim 10^8$ cm^{-2} s^{-1} on the far side and decrease it by an additional 20% on the near side.

With increasing latitude the geometric influx of solar wind on the surface tends to decay as the cosine of latitude. At the near side equator, the ratio of fluxes of solar wind and molecular rain is $\sim$ 6000 : 1, at 80°latitude the ratio is $\sim$ 1000 : 1. A case on point is the comparable abundances of trapped solar wind ^{4}He, ^{20}Ne, and ^{36}Ar in Apollo 16 soils collected from permanent shadow near House Rock and those in soils collected from exposed regolith nearby (Eberhardt et al., 1976). The clear implication is that over most of the polar regions, including cold traps, the ratio of solar wind and molecular rain fluxes are affected more by topography than latitude, with poleward-facing slopes retaining excessive amounts of adsorbed meteoritic water.

Some indirect guidance regarding sputtering of adsorbed water by solar wind ions can be obtained from the solar wind sputter simulations of Wurz et al. (2007) for a variety of lunar soils. Briefly, Wurz et al. found total sputter yields of 4-7% for oxygen and lesser amounts for other elements. They also noted that "practically all" species are ejected with super-escape speeds. Based on the difference in binding energies of solid molecular structures and of sorption, the sputter yield should be at least 10% for water that desorbs at less than half of the solidus temperature. In other words, the rate of solar wind scouring of grain surfaces is more than 100-fold greater than monolayer acquisition of meteoritic water.

Recently, Honnibal et al. (2021) reported on the detection of lunar surface water at an exposed, sunlit high latitude location. They concluded that the water had to be bound in glass or sequestered from the local harsh environmental elements. Due to the reduction in solar wind sputtering losses, the scenario presented here might also give rise to an enhanced near-surface abundance of water bound by the Ca-H exchange.

4 Conclusions

The key experimental finding of this report is that the LADEE data show no evidence of exospheric water on the moon. More important, the upper bound for exospheric water falls short by several orders of magnitude of allowing the exosphere to be the conduit for transferring the meteoritic water influx to polar cold traps. This conclusion shifts the lunar water problem from polar sequestration to one of identifying the process or pro-

cesses that remove meteoritic water from the moon. The elements of the hypothesis presented here are that:

1. Isolated meteoritic H_2O molecules are chemically adsorbed by reversible cation exchange.
2. Adsorbed meteoritic water escapes from the moon due to solar wind scouring of exposed surfaces.
3. The amorphous rims on soil grains become hydrous phyllosilicates when adsorbed H_2O molecules happen to congregate.
4. The rims hold part or all of the OH in lunar soils reported by Clark (2009), Pieters et al. (2009), and Sunshine et al. (2009).
5. The cation exchange scenario may be consistent with the recent 6 micron IR observations by Honnibal et al. (2021), although more observations are required.

Acknowledgments
This work was in part supported by the NASA Solar System Exploration Research Virtual Institute.

Open Research

The actual data set used in this investigation was assembled by the first author during the LADEE mission. It is identical to the raw data set that is publicly available at the Planetary Data System (http://pds-atmospheres.nmsu.edu/data_and_services/atmospheres_data/LADEE/nms.html).

References

Arnold, J. R. (1979). Ice in the lunar polar regions. *J. Geophys. Res.*, *84*, 5659–5668.

Bernatowicz, T. J., & Podosek, F. A. (1991). Argon adsorption and the lunar atmosphere. *Proc. Lunar Planet Sci. Conf. 21*, 306–313.

Bibring, J. P., Duraud, J. P., Durrieu, L., Jouret, C., Maurette, M., & Meunier, R. (1972). Ultrathin amorphous coatings on lunar dust grains. *Science*, *175*, 753–755.

Bischoff, A., & Geiger, T. (1995). Meteorites from the sahara: Find locations, shock classification, degree of weathering and pairing. *Meteoritics (ISSN 0026-1114)*, *30*(1), 113–122.

Borin, P., Cremonese, G., Marzari, F., & Lucchetti, A. (2017). Asteroidal and cometary dust flux in the inner solar system. *A and A*, *605*(A94). doi: 10.1051/0004-6361/201730617

Clark, N. (2009). Detection of adsorbed water and hydroxyl on the moon. *Sciencexpress*. doi: 10.1126/science.1178105

Cremonese, G., Borin, P., Lucchetti, A., Marzari, F., & Bruno, M. (2013). Micrometeoroids flux on the moon. *A and A*, *551*(A27). doi: 10.1051/0004-6361/201220541

Eberhardt, P., Eugster, O., Geiss, J., Grögler, N., Guggisberg, S., & Mörgeli, M. (1976). Noble gasses in the apollo 16 special soils from the east-west split and the permanently shadowed area. *Proc. Lunar Sci. Conf. 7th*, 563–585.

Epstein, S., & Taylor, H. P. (1971). O^{18}/O^{16}, Si^{30}/Si^{28}, D/H, and C^{13}/C^{12} ratios in lunar samples. *Proc. Lunar Sci. Conf, 2nd*, 1421–1441.

Epstein, S., & Taylor, H. P. (1972). O^{18}/O^{16}, Si^{30}/Si^{28}, C^{13}/C^{12} and D/H studies of apollo 14 and 15 samples. *Proc. Lunar Sci. Conf, 3nd*, 1429–1454.

Epstein, S., & Taylor, H. P. (1973). The isotopic composition and concentration of

water, hydrogen, and carbon in some apollo 15 and 16 soils and in the apollo 17 orange soil. *Proc. Lunar Sci. Conf, 4th*.

Epstein, S., & Taylor, H. P. (1974). D/H and $^{18}O/^{16}O$ ratios in the "rusty" breccia 66095 and the origin of "lunar water. *Proc. Lunar Sci. Conf, 5th*, 1839–1854.

Epstein, S., & Taylor, H. P. (1975). Investigation of the carbon, hydrogen, oxygen, and silicon isotope concentration relationships on the grain surfaces of a variety of lunar soils and in some apollo 15 and 16 core samples. *Proc. Lunar Sci. Conf, 6th*, 1771–1798.

Hodges, R. R. (1972). Applicability of a diffusion model to lateral transport in the terrestrial and lunar exospheres. *Planet. Space Sci.*, *20*, 103–115.

Hodges, R. R. (1980). Lunar cold traps and their influence on argon-40. *Proc. Lunar Sci. Conf., 11th*, 2463 –2477.

Hodges, R. R. (1991). Exospheric transport restrictions on water ice in lunar polar traps. *Geophys. Res. Lett.*, 2113–2116.

Hodges, R. R. (2002). Ice in lunar polar regions revisited. *J. Geophys. Res.*, doi: 10.1029/2000JE001.

Hodges, R. R. (2016). Methane in the lunar exosphere: Implications for solar wind carbon escape. *Geophys. Res. Lett.*, *43*, 6742–6748. doi: 10.1002/2016GL068994

Hodges, R. R. (2018). Semiannual oscillation of the lunar exosphere: Implications for water and polar ice. *Geophys. Res. Lett.*, *45*. doi: 10.1029/2018GL077745

Hodges, R. R., Hoffman, J. H., & Johnson, F. S. (1973). Composition and dynamics of the lunar atmosphere. *Proc. Lunar Sci. Conf., 4th*, 2855 –2864.

Hodges, R. R., & Johnson, F. S. (1968). Lateral transport in planetary exospheres. *J. Geophys. Res.*, *73*, 7307–7317.

Hodges, R. R., & Mahaffy, P. R. (2016). Synodic and semiannual oscillations of argon-40 in the lunar exosphere. *Geophys. Res. Lett.*, *43*, 22–27. doi: 10.1002/2015GL067293.

Honnibal, C. I., Lucey, P. G., & et al., S. L. (2021). Molecular water detected on the sunlit moon by SOFIA. *Nat Astron*, *5*, 121–127. doi: 10.1038/s41550-020-01222-x

Housley, R. M. (1977). Solar wind and micrometeorite effects in the lunar regolith. *Philosophical Transactions of the Royal Society of London, A*, *285*, 363–367. doi: 10.1098/rsta.1977.0075

Mahaffy, P. R., Hodges, R. R., & et al., M. B. (2014). The neutral mass spectrometer on the Lunar Atmosphere and Dust Environment Explorer mission. *Space Sci Rev*, *185*, 27–61. doi: 10.1007/s11214-014-0043-9

Pieters, C. M., Goswami, J. N., & et al., R. N. C. (2009). Character and spatial distribution of OH/H_2O on the surface of the moon seen by M^3 on Chandrayaan-1. *Sciencexpress*. doi: 10.1126/science.1178658

Sunshine, J. M., Farnham, T. L., & et al., L. M. F. (2009). Temporal and spatial variability of lunar hydration as observed by the deep impact spacecraft. *Sciencexpress*. doi: 10.1126/science.1179788

Watson, K., Murray, B. C., & Brown, H. (1961). The behavior of volatiles on the lunar surface. *J. Geophys. Res.*, *66*, 3033–3045.

Wurz, P., Rohner, U., & et al., J. A. W. (2007). The lunar exosphere: The sputtering contribution. *Icarus*, *191*, 486–496. doi: 10.1016/j.icarus.2007.04.034